

A tissue equivalent phantom for simultaneous near-infrared optical tomography and EEG

R. J. Cooper,* R. Eames, J. Bruncker, L. C. Enfield, A. P. Gibson, and Jeremy C Hebden

Department of Medical Physics and Bioengineering, University College London, London, WC1E 6BT, UK

**rcooper@medphys.ucl.ac.uk*

Abstract: We describe a phantom which enables EEG and near-infrared optical tomography to be performed simultaneously over the same volume. The phantom provides a surface electrical contact impedance comparable to that of the human scalp, whilst also possessing an optical scattering coefficient and electrical conductivity equivalent to that of brain tissue. The construction of the phantom is described, as is the resulting simultaneous EEG and near infrared optical tomography experiment, which, to our knowledge, is the first performed on a scale comparable to that of the infant human brain. This imaging experiment successfully shows the suitability of this phantom construction for the assessment of simultaneous EEG and near infrared optical tomography systems.

©2010 Optical Society of America

OCIS codes: (170.0110) Imaging systems; (170.6960) Tomography.

References and links

1. J. Gotman, E. Kobayashi, A. P. Bagshaw, C. G. Bénar, and F. Dubeau, "Combining EEG and fMRI: a multimodal tool for epilepsy research," *J. Magn. Reson. Imaging* **23**(6), 906–920 (2006).
2. R. I. Goldman, J. M. Stern, J. Engel, Jr., and M. S. Cohen, "Simultaneous EEG and fMRI of the alpha rhythm," *Neuroreport* **13**(18), 2487–2492 (2002).
3. H. Obrig, H. Israel, M. Kohl-Bareis, K. Uludag, R. Wenzel, B. Müller, G. Arnold, and A. Villringer, "Habituation of the visually evoked potential and its vascular response: implications for neurovascular coupling in the healthy adult," *Neuroimage* **17**(1), 1–18 (2002).
4. S. P. Koch, J. Steinbrink, A. Villringer, and H. Obrig, "Synchronization between background activity and visually evoked potential is not mirrored by focal hyperoxygenation: implications for the interpretation of vascular brain imaging," *J. Neurosci.* **26**(18), 4940–4948 (2006).
5. M. C. Toet, and P. M. Lemmers, "Brain monitoring in neonates," *Early Hum. Dev.* **85**(2), 77–84 (2009).
6. F. Wallois, A. Patil, G. Kongolo, S. Goudjil, and R. Grebe, "Haemodynamic changes during seizure-like activity in a neonate: a simultaneous AC EEG-SPIR and high-resolution DC EEG recording," *Neurophysiol. Clin.* **39**(4–5), 217–227 (2009).
7. M. S. Scher, "Neonatal seizures and brain damage," *Pediatr. Neurol.* **29**(5), 381–390 (2003).
8. A. P. Gibson, T. Austin, N. L. Everdell, M. Schweiger, S. R. Arridge, J. H. Meek, J. S. Wyatt, D. T. Delpy, and J. C. Hebden, "Three-dimensional whole-head optical tomography of passive motor evoked responses in the neonate," *Neuroimage* **30**(2), 521–528 (2006).
9. R. J. Cooper, N. L. Everdell, L. C. Enfield, A. P. Gibson, A. Worley, and J. C. Hebden, "Design and evaluation of a probe for simultaneous EEG and near-infrared imaging of cortical activation," *Phys. Med. Biol.* **54**(7), 2093–2102 (2009).
10. B. W. Pogue, and M. S. Patterson, "Review of tissue simulating phantoms for optical spectroscopy, imaging and dosimetry," *J. Biomed. Opt.* **11**(4), 041102 (2006).
11. R. J. Cooper, D. Bhatt, N. L. Everdell, and J. C. Hebden, "A tissue-like optically turbid and electrically conducting phantom for simultaneous EEG and near-infrared imaging," *Phys. Med. Biol.* **54**(18), 403–408 (2009).
12. T. Tidswell, A. Gibson, R. H. Bayford, and D. S. Holder, "Three-dimensional electrical impedance tomography of human brain activity," *Neuroimage* **13**(2), 283–294 (2001).
13. F. E. W. Schmidt, M. E. Fry, E. M. C. Hillman, J. C. Hebden, and D. T. Delpy, "A 32-channel time-resolved instrument for medical optical tomography," *Rev. Sci. Instrum.* **71**(1), 256–265 (2000).
14. S. R. Arridge, J. C. Hebden, M. Schweiger, F. E. Schmidt, M. E. Fry, E. M. Hillman, H. Dehghani, and D. T. Delpy, "A method for three-dimensional time-resolved optical tomography," *Int. J. Imaging Syst. Technol.* **11**(1), 2–11 (2000).

1. Introduction

The application of dual-modality imaging techniques to the study of human brain function has become increasingly common in the last decade. Functional imaging techniques can be broadly placed into two categories: the first contains electroencephalography (EEG) and magnetoencephalography (MEG), which directly measure the electromagnetic dynamics of groups of active neurons. The second contains functional magnetic resonance imaging (fMRI), positron emission tomography (PET), single photon emission computed tomography (SPECT) and near-infrared spectroscopy (NIRS) and imaging, all of which use some metabolic variation as a proxy measure of neuronal activation. Dual-modality functional imaging provides the greatest amount of complementary information when one technique is chosen from each of these two fundamental categories. This allows for direct investigation of the relationship between neuronal activation and the given metabolic proxy, and often has the advantage of producing a significantly improved spatio-temporal resolution.

EEG-fMRI is fast becoming a standard technique and has been used to study many forms of human brain function and disorder, including resting state brain function, functional processing, epilepsy and neuro-vascular coupling, despite the significant technical challenges associated with the technique [1,2]. Simultaneous EEG and NIR methods have also proved to be of considerable interest, not least because these techniques are relatively inexpensive, mutually compatible and applicable at the bedside. EEG-NIRS has already been applied in a variety of studies of functional processing in adults and children, including studies of resting state, visual processing and neurovascular coupling [3,4]. However, it has become apparent that one of the most significant applications of simultaneous EEG and NIR techniques will be to neonatal medicine. Preliminary studies suggest that the simultaneous observation of electrocortical and haemodynamic variations in the newborn has the potential to provide new insight into certain encephalopathies, and may well aid clinical diagnosis [5,6]. Neonatal seizure, while often a symptom of underlying brain injury, is thought to cause significant neurological damage [7] but remains difficult to diagnose and monitor. Amplitude-integrated EEG remains the gold standard diagnostic technique for neonatal seizure, despite the significant issue of whether EEG (particularly in the limited electrode arrangements applied clinically) is sensitive to neuronal hyperactivity and synchronicity in sub-cortical regions of the brain. The simultaneous use of EEG and optical techniques, particularly in an arrangement that provides sensitivity to haemodynamic events in deeper regions of the brain, has the potential to address this issue. Optical tomography is able to produce whole-head, three-dimensional images of changes in concentration of oxy and de-oxyhaemoglobin of the neonatal brain [8] and we anticipate that EEG-optical tomography will become an effective new method for the study and diagnosis of neonatal encephalopathies.

EEG and NIR techniques are mutually compatible; the recording of one does not inherently affect the recording of the other. As a result the most significant challenge in the simultaneous application of these two techniques is the coupling of the necessary EEG electrodes and optical fibre bundles to the scalp. We have designed a combined electrode/optical fibre bundle ('opto-electrode') which is easy to apply in the clinical environment and minimises the occupied area of the scalp, thus maximising our possible sampling density [9]. In order to assess the suitability of this (and other) probe designs, it was necessary to produce a tissue-mimicking phantom. A broad variety of tissue-equivalent phantoms have been developed to evaluate optical imaging systems [10]. However, for the purposes of EEG-optical tomography, we require a phantom that possesses tissue-like optical properties, that provides a source of varying electrical potential difference (equivalent to that measured at the scalp by EEG) and that can be imaged in three-dimensions. We previously described a phantom which allowed simultaneous EEG and planar optical topography [11]. In this note we describe a new design of phantom appropriate for simultaneous EEG and 3D optical tomography. This will enable dual-modality image reconstruction paradigms to be

developed and tested prior to implementation of EEG-optical tomography to the study of neonatal seizure.

2. Phantom Design

The EEG-optical tomography phantom is designed around a hollow cylindrical container, 70 mm in diameter and 110 mm in height. This container is constructed from a polyester resin (Alec Tiranti Ltd., UK), which is made optically turbid by the addition of superwhite resin pigment (Alec Tiranti Ltd., UK). In order to make this solid cylindrical container electrically conducting, a dense array of 8 mm long, 0.25 mm diameter gold-plated copper wires (Griffin, Germany) is embedded in the resin so as to span the thickness of the container wall. These lengths of wire are spaced 2.5 mm apart around the surface of the cylindrical mould so as to form a ring. Five such rings, vertically spaced by 2.5 mm, form a conductive band, 10 mm high, around the middle of the cylindrical container (see Fig. 1). The walls of the cylinder are 5 mm in thickness and the gold-plated copper wires positioned flush with the external surface of the container, whilst protruding by 3 mm from the internal surface of the container. The density and size of the wire array was chosen as a result of a previous design, which indicated that such an array would provide an electrical contact impedance at the surface of the phantom comparable to that of the human scalp. Arranged in this fashion, the wires in the phantom lie parallel to the optical path of the NIR light coupled in to and out of the phantom for optical tomographic imaging, and as these wires are very fine, it is assumed that they do not significantly influence the optical characteristics of the phantom.

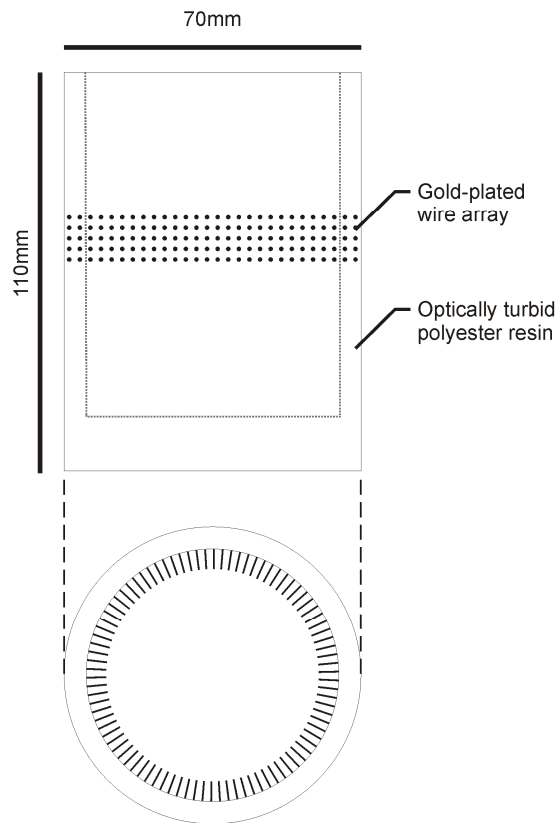


Fig. 1. The design of the cylindrical, optically turbid and electrically conducting phantom.

The phantom is completed by filling the optically turbid, electrically conducting cylindrical container with an aqueous solution containing a scattering agent (Intralipid at 1%

by volume) and sodium chloride (at 0.2% by mass). In order to provide a target for optical tomography and a source of a time-varying electrical potential difference for EEG recording, a current dipole embedded in an optically-absorbing medium is introduced into the phantom solution. This target consists of two silver/silver-chloride pellet electrodes, 2 mm in diameter, spaced 5 mm apart and embedded in a polyester resin cylinder 10 mm in diameter. This resin target is provided with the same reduced scattering coefficient as the solution, but with an increased optical absorption coefficient obtained by the addition of Pro-jet dye (Avecia Inc. USA). The pellet electrodes are connected to the output terminals of a signal generator, which produces an 11 Hz sine wave with a peak-to-peak amplitude of 40 mV. This amplitude was found to produce variations in electrical potential difference at the phantom surface of around 20 μ V, comparable in amplitude to in-vitro EEG recordings.

The resulting phantom has a reduced scattering coefficient of 1 mm^{-1} throughout and absorption coefficients of 0.001 mm^{-1} , 0.002 mm^{-1} and 0.04 mm^{-1} in the phantom wall, the aqueous solution and the target respectively (all as measured at 800 nm). The value of the absorption coefficient in the body of this novel phantom is lower than that of human tissue, but as the phantom is designed to enable imaging of a change in optical properties, this will not affect the fundamental outcome of a simultaneous EEG-optical tomography experiment and can easily be amended in future versions.

The addition of salt to the phantom solution renders the electrical conductivity across its volume equivalent to that of brain tissue [12]. The contact impedance of the phantom surface was measured across 12 random locations around the conduction band using standard clinical electrodes and was found to average 26.4 k Ω at 10 Hz. This is higher than the benchmark value for abraded scalp of around 5 k Ω and different to previous designs probably due to the curvature of the phantom surface. However, electrode contact impedance can be made arbitrarily small by increasing the contact area of the gold-coated copper wires at the external surface of the phantom using, for example, a conductive paint. The phantom design is shown in Fig. 1.

3. Simultaneous EEG and NIR optical tomography

In order to validate the phantom design, a simultaneous EEG and NIR optical tomography experiment was performed using an array of twelve opto-electrodes [9] evenly spaced around the external circumference of the phantom at the level of the conductive band. Each of these opto-electrodes acted as an active EEG recording electrode whilst a standard reference electrode was placed in contact with the aqueous solution. The optically-absorbing, current dipole target was position level with the conductive band, 52 mm from the centre of the phantom, as shown in Fig. 2a.

EEG data were recorded using twelve channels of a Grass-Telefactor H2O 32-channel EEG recording system (Grass Technologies, Astro-Med Inc.) with a sample rate of 400 Hz. As the phantom uses a sinusoidal signal generator to mimic an EEG source, the level of broadband noise is essentially irrelevant, and the EEG filters could be set to produce as narrow a pass-band as possible, in this case between 10 and 12 Hz. Data were acquired using the software package EEG TWin 2.6 (Grass Technologies, Astro-Med Inc.), and then analyzed offline using Matlab (The Mathworks Inc., USA) and EEGLab (SCCN, UC San Diego, USA). EEGLab was used to produce a topographic representation and a current dipole reconstruction of the recorded EEG data.

Optical tomographic data were obtained using a 32-channel time domain imaging system [13]. This system produces light pulses with a duration of 2 ps at 780 and 815 nm which are coupled sequentially to the object under investigation via a set of optical fibre connectors. Each connector consists of a detector fibre bundle and a source fibre arranged co-axially. Diffusely scattered NIR light from the illuminated medium is detected using a series of microchannel plate PMTs, which, in conjunction with timing electronics and variable attenuators to prevent overexposure, enable the time of flight of each detected photon to be

recorded. For this experiment, only twelve channels and connectors were required, each coupled to the ring-array via an opto-electrode probe. One complete data set was obtained prior to the target being inserted into the phantom in order that an image of the change in optical absorption could be obtained. Images of the change in optical absorption coefficient were reconstructed using the time-resolved optical absorption and scatter tomography (TOAST) reconstruction package developed at UCL [14]. TOAST uses the finite element method to discretely model the diffusion approximation to the radiative transfer equation, which governs light propagation in diffusive media. Images are reconstructed iteratively by adjusting the optical properties of the finite element mesh to minimise the differences between modelled and recorded data. In this case, the initial optical properties were set to equal those of the aqueous phantom solution (i.e. an absorption coefficient of 0.002 mm^{-1} and a reduced scattering coefficient of 1 mm^{-1}). A cylindrical mesh was used to reconstruct 2D images of absorption and reduced scatter. Images of the difference in absorption coefficient at 780 and 815 nm were reconstructed, using a data set from the homogenous phantom as reference measurements. The 10th iteration was analysed as this was found to be the number beyond which no further improvement to the images was observed.

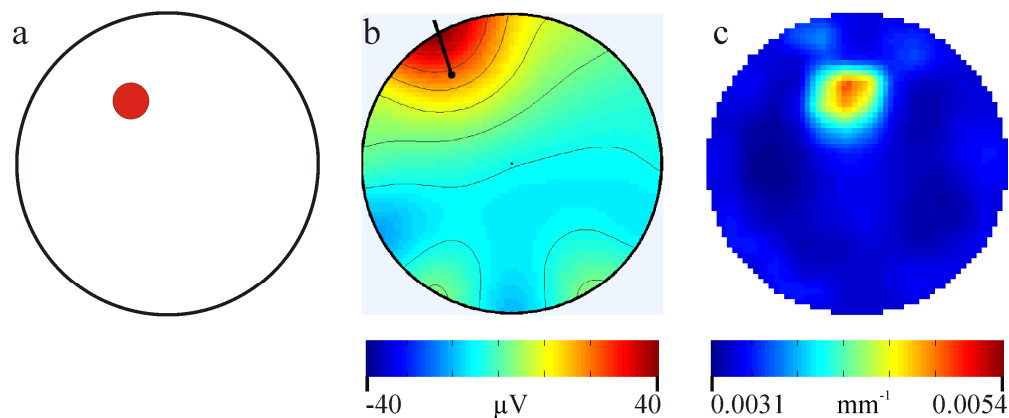


Fig. 2. The actual phantom geometry is shown in Fig. 2a, the red circle indicating the location of the optically absorbing, current-dipole target. Figure 2b show the topography of the re-scaled, dominant independent component of the recorded EEG data and the resulting dipole reconstruction. Figure 2c shows the reconstructed image of change in optical absorption coefficient at 780nm.

4. Results

Figure 2a shows the experimental phantom geometry, with the red circle representing the size, and position of the optically absorbing current dipole target. Figure 2b shows the topography of the first independent component of the EEG data and the result of the current dipole localisation. The error of the reconstructed dipole position is 8.1 mm. An accurate dipole localisation is to be expected given the electrical isotropy of the phantom. Figure 2c shows the reconstructed tomographic image of change in optical absorption coefficient at 780 nm. The focal change in reconstructed absorption coefficient is accurately located, at 3.3 mm from the actual target position. The dimensions of the focal change are also similar to that of the actual target, with a full-width at half maximum of 11.3 mm.

5. Discussion

In this paper we have sought to illustrate the efficacy of our electrically conducting, tissue-equivalent EEG-optical tomography phantom. The design described here is inexpensive, portable, re-usable and relatively easy to build. A phantom which simplifies and standardises the testing of combined EEG-optical tomography systems will be of real benefit as interest in

this promising combined imaging modality continues to grow. This phantom (and more complex versions of it, which may incorporate a series of layers of varying conductivity so as to further mimic the tissue of the head and brain) will also aid the optimisation of image reconstruction methods. Specifically, we envisage that such phantoms will play a significant role in the testing of software paradigms which enable EEG source localisation to be constrained by simultaneously recorded optical tomography images.